Environmental Science & Technology

pubs.acs.org/est

Article

Environmental Risk of Arsenic Mobilization from Disposed Sand Filter Materials

Anh Van Le, E. Marie Muehe, Soeren Drabesch, Juan Lezama Pacheco, Timm Bayer, Prachi Joshi, Andreas Kappler, and Muammar Mansor*

Cite This: *Environ. Sci. Technol.* 2022, 56, 16822−16830

Read Online

ACCESS | Metrics & More | Article Recommendations | Supporting Information

ABSTRACT: Arsenic (As)-bearing water treatment residuals (WTRs) from household sand filters are usually disposed on top of floodplain soils and may act as a secondary As contamination source. We hypothesized that open disposal of these filter-sands to soils will facilitate As release under reducing conditions. To quantify the mobilization risk of As, we incubated the filter-sand, the soil, and a mixture of the filter-sand and soil in anoxic artificial rainwater and followed the dynamics of reactive Fe and As in aqueous, solid, and colloidal phases. Microbially mediated Fe(III)/As(V) reduction led to the mobilization of 0.1−4% of the total As into solution with the highest As released from the mixture microcosms equaling 210 μg/L. Due to the filter-sand and soil interaction, Mössbauer and X-ray absorption spectroscopies indicated that up to 10% Fe(III) and 32% As(V) were reduced in the mixture microcosm. Additionally, the mass concentrations of colloidal Fe and As analyzed by single-particle ICP-MS decreased by 77−100% compared to the onset of reducing conditions with the highest decrease observed in the mixture setups (>95%). Overall, our study suggests that (i) soil provides bioavailable components (e.g., organic matter) that promote As mobilization via microbial reduction of As-bearing Fe(III) (oxyhydr)oxides and (ii) As mobilization as colloids is important especially right after the onset of reducing conditions but its importance decreases over time.

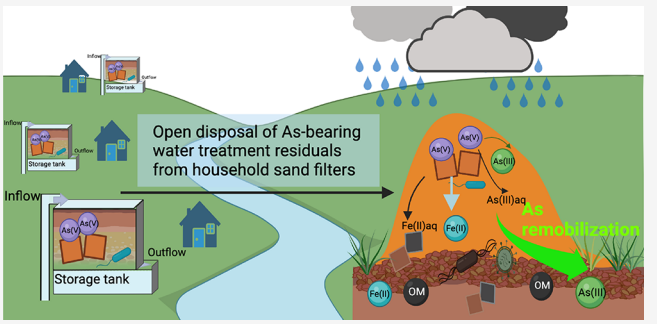

KEYWORDS: *arsenic-bearing water treatment residuals, open disposal, disposed filter-sand, microbial reduction, colloidal transport, arsenic remobilization*

INTRODUCTION

Drinking water treatment facilities generate vast quantities of residuals that are filled with contaminants.[1,2] These water treatment residuals (WTRs) are commonly discharged in landfills in regions with sufficient space and resources.[3,4] However, in As-affected areas in rural South Asia, management of As-bearing WTRs is poor, leading to the open disposal of As-bearing WTRs to ponds, rivers, and soils without any site preparation.[5,6] A problem in the management of As-bearing WTRs is inadequate testing procedures that are not representative of actual conditions in the disposal sites, thus leading to over- or underprediction of As remobilization.[4] Common leach tests, such as the toxicity characteristic leaching procedure (TCLP), have been shown to underpredict As mobilization from WTRs in landfills[7,8] since the tests do not account for microbial activities that change over long periods and redox fluctuations.[3,4] A recent study indicated that open disposal strategies especially pose the highest potential risk to the environment and human health.[6]

In the Red River delta in Vietnam, household sand filters are regularly used to remove toxic As from groundwater for drinking purposes. The groundwater is filtered through a reactive sand layer by gravity in which Fe and As co-oxidize and precipitate on the sand matrix.[9−11] Eleven million people rely on household sand filters in Vietnam (data in 2007).[12,13] With an average of 3.5 people per household (reported in 2009),[14] this means that around 3.1 million households use sand filters. The implication of this is that around 2.1 × 10^5 tons of sand filter residues is openly disposed to the environment every six months (assuming a 0.47 m^2 surface area, 1470 kg/m^3 density, 35% porosity, 10 cm of sand layer disposed every 6 months).[9] The As mobilization risk from these staggering amounts of materials has yet to be investigated. Other As contaminated sources from mining waste were previously reported to cause pollution to soil and crops around the disposal area.[15,16]

Received: July 8, 2022
Revised: October 15, 2022
Accepted: October 27, 2022
Published: November 9, 2022

The mobilization risk of As from the filter-sand is influenced by redox alteration. Under toxic conditions, arsenic primarily exists as oxidized As(V) adsorbed to Fe(III) (oxyhydr)oxides.[9] During the monsoon season with frequent and heavy rainfall and potential flood events, the disposed filter-sand turns anoxic and reducing, leading to a high risk of As release to porewater. The general accepted mechanisms of As mobilization are via microbial reduction of As-bearing Fe(III) (oxyhydr)oxides[17,18] as well as the direct reduction of As(V) to As(III) by As-reducing bacteria (AsRB).[19] As(III) has a lower adsorption affinity to Fe(III) (oxyhydr)oxides than As(V) and is thus more amenable to mobilization.[20]

Open disposal of the As-contaminated filter-sand material to the topsoil leads to mixing with the complex soil matrix that contains diverse microbial communities, organic matter (OM), and minerals (e.g., Fe−Al−Mn (oxyhydr)oxides). The interaction between the disposed filter-sand (enriched with As) and soil therefore potentially plays a crucial but poorly understood role in the fate of As. Another factor to consider is whether disposed filter-sand is mobilized in the form of colloids, which is similar to the transport mechanism of other toxic contaminants in natural waters.[21] We define colloids as small particles subject to suspension and mobilization; this definition encompasses particles with size ranges that are beyond the traditionally considered 1-μm size cutoff.[22] An increase of mobilized colloidal Fe(III) (oxyhydr)oxides can further facilitate As(V) transport.[23,24] At the same time, colloidal Fe(III) (oxyhydr)oxides are known to be more susceptible to microbial reduction than larger mineral aggregates, therefore possibly promoting solubilization of As-bearing colloidal Fe(III) minerals.[25−27] Thus, it is crucial to also consider colloid-facilitated transport of As to fully evaluate the risk of As mobilization.[28−30]

In this study, we performed microcosm experiments in which As-bearing WTRs from the filter-sand, soil, and mixture of the filter-sand and soil were incubated under reducing conditions over 130 days. We followed changes in reactive Fe(II), Fe minerals, As redox states, and coordination environments in the solid phase and the dynamics of dissolved and colloidal Fe and As over time. The results allowed us to assess the mobilization risk of As from open disposal of the sand filter material.

MATERIALS AND METHODS

Field Site and Sample Collection. We collected disposed filter-sand materials from several household filters in Tu Nhien village (20.848518 N, 105.919483 E), around 25 km Southeast of Hanoi, Vietnam, inside the meander of the Red River. Soil samples (top 20 cm) were collected from several gardens in the same village; we collected soils that were not in contact before with the disposed filter material. The filter-sand and floodplain soils were collected in five independent replicates, immediately cooled on ice during transport, and stored at 4 °C. In the laboratory, the filter-sand or floodplain soils were used alone (100%) or mixed in a ratio of 1:1 before being used for incubation experiments.

Filter-Sand and Soil Sample Characterization. The elemental composition (Fe, Al, P, As, and Mn) of the disposed filter-sand, floodplain soil, and mixture of filter-sand and soil were analyzed by microwave digestion followed by inductively coupled plasma mass spectrometry analysis (ICP-MS) (Agilent 7900, Agilent Technologies). After drying in the oven (105 °C), 0.5 grams of the sample was added to 12 mL of aqua-regia solution (9 mL of 37% HCl and 3 mL of 65% HNO_3) in Xpress Plus Teflon vessels. The samples were digested in the Microwave Accelerated Reaction System, MARS 6 (CEM, USA), with further details in Section S1.

For total organic carbon (TOC) quantification, samples were dried at 60 °C, grounded, and analyzed in triplicate with a soliTOC cube (Elementar Analysensysteme GmbH, Germany).

Microcosm Experiments. Microcosms were set up by adding 12.5 g of the disposed filter-sand, or soil, or pre-mixed 1:1 filter-sand and soil into 125 mL of sterile anoxic artificial rainwater (ARW; Table S1 and Section S2) within 250 mL serum bottles. Thus, the solid:liquid ratio is 1:10 in all bottles. The initial pH of all microcosms ranged from 6.8 to 7.3 (Table 1). Additionally, abiotic controls were amended with 160 mM sodium azide (NaN_3) to inhibit microbial respiration. All microcosms were prepared in triplicate in an anoxic glovebox (100% N_2, <30 ppm O_2, MBRAUN UNIlab). The microcosms were kept standing vertically at 28 °C in the dark without shaking until analysis.

Table 1. Elemental Compositions of the Floodplain Soil, Disposed Filter-Sand Material, and Mixture of the Filter-Sand and Soil Prior to Incubation (All Samples Were Analyzed in Triplicate)

	floodplain soil	disposed filter-sand material	mixture of filter-sand and soil
Fe (g/kg)	50 ± 4	97 ± 6	76 ± 8
Al (g/kg)	79 ± 6	22 ± 2	55 ± 6
P (g/kg)	1 ± 0.1	5 ± 0.5	3 ± 0.3
As (mg/kg)	29 ± 3	1441 ± 81	725 ± 64
Mn (mg/kg)	1166 ± 92	539 ± 52	911 ± 153
Fe/Mn ratio	42.5 ± 0.1	182.4 ± 28.3	84.3 ± 6.3
Fe/As ratio	1723 ± 39	67.5 ± 0.6	105 ± 3
TOC (g/kg)	11.7 ± 0.4	3.2 ± 0.2	7.2 ± 0.2
initial pH[a]	6.8	7.3	7.2

[a]Initial pH values of the microcosms.

Solution Chemistry Analysis. Immediately before sampling, the microcosms were homogenized by shaking. Aliquot suspensions (3 mL) were collected in two 2 mL Eppendorf tubes (1.5 mL in each) and centrifuged for 15 min at 12,100g in the glovebox. The supernatants were filtered (0.22 μm cellulose filter, EMD Millipore) and diluted with 1% HNO_3 for quantification of dissolved Fe and As by ICP-MS. Sediment pellets remaining after centrifugation were extracted with either (a) 1 mL of 0.5 M HCl for 2 h (to quantify bioavailable/poorly crystalline Fe) or (b) 1 mL of 6 M HCl for 24 h (to quantify crystalline Fe).[31] Afterward, all samples were centrifuged for 15 min at 12,100g, and 100 μL of the supernatant was collected and diluted 10-fold with 1 M HCl before analysis. HCl-extractable Fe(II) and Fe (total) were quantified spectrophotometrically using the ferrozine assay.[32,33]

Iron Mineral Analysis Using Mössbauer Spectroscopy. Mössbauer spectroscopy was used to identify Fe minerals. Pre-incubation samples were loaded as dried powders into 1 cm^2 Plexiglas holders. Solids from the microcosms collected by filtration (0.45 μm nitrocellulose filter, Millipore) were fixed

https://doi.org/10.1021/acs.est.2c04915
Environ. Sci. Technol. 2022, 56, 16822−16830

between two pieces of Kapton tape in the glovebox and kept frozen and anoxic at −20 °C in a sealed bottle until measurement. Spectra were collected at 77 and 5 K using a constant acceleration drive system (WissEL) in the transmission mode with a ^{57}Co/Rh source. Analyses were carried out using a Recoil (University of Ottawa) and the Voigt Based Fitting (VBF) routine.[34]

X-ray Absorption Spectroscopy (XAS). To identity As redox states and binding environments, samples were collected from the microcosms prior to incubation and then freeze-dried, ground, and stored anoxically until measurement. Reference model compounds were synthesized in an anoxic glovebox by adsorbing arsenate ($Na_2HAsO_4{\cdot}7H_2O$, Sigma-Aldrich) and arsenite ($AsNaO_2$, Sigma-Aldrich) onto ∼30 mg of freshly prepared 500 mM ferrihydrite[35] in a molar ratio of 30:1 for 10 h with gentle overhead mixing. Model compounds were washed twice in anoxic MQ water, freeze-dried, ground, and diluted with approximately 26 mg of boron nitride and stored anoxically until measurement. Samples and standards were placed in aluminum sample holders (3 mm by 13 mm window) and sealed with 0.5 mil Kapton tape from both sides. Arsenic K-edge extended X-ray absorption fine structure (EXAFS) data were obtained at beamline 7−3 at Stanford Synchrotron Radiation Lightsource (SSRL), Menlo Park, USA. Spectra were collected in the fluorescence detection mode using a 30-element germanium detector array using a reference gold foil in the transmission detection mode and calibrating to 11,919 eV. More details on beamline settings are given in Section S3. Data were deadtime-corrected and averaged with Sixpack,[36] and repetitive scans were aligned, merged, truncated, deglitched, normalized to an edge step of one, and background-subtracted in Athena.[37] To verify data, XANES (extracted from EXAFS) and EXAFS data were analyzed for As speciation differences. Principle components (PCA) and target transforms were analyzed for merged scans followed by least-square fitting by linear combination (LCF) of the synthesized model compound spectra.[38] EXAFS were analyzed to a k of 12. The LCF components are estimated to be accurate at 10%, and the detection limit of the contributing components is set to 10%.[39,40] Shell-by-shell fitting was performed to support LCF fits, as given in Section S3.

Quantification of Fe and As in Colloidal Fractions. Microcosms were shaken, and large particles were allowed to settle for 24 h while standing in the glove box. Afterward, about 0.1 mL of suspension was carefully sampled directly from the top and stored anoxically at 4 °C. The suspensions were diluted 1000-fold in anoxic H_2O in a Falcon tube in the glove box and taken out right before the analysis. All samples were analyzed in a time-resolved analysis mode on an Agilent 7900 ICP-MS instrument.[30] More details are provided in Section S4.

RESULTS AND DISCUSSION

Characterization of the Disposed Filter-Sand and Floodplain Soil Prior to Incubation Experiments. Microwave digestion and TOC analyses were performed to quantify elemental (Fe, Al, P, As, Mn) and organic carbon contents. The samples contained 50−100 g/kg of Fe, 22−80 g/kg of Al, 1−5 g/kg of P, 29−1440 mg/kg of As, 540−1166 mg/kg of Mn, and 2−12 g/kg of TOC (Table 1). The filter-sand material was rich in Fe, P, and As relative to the soil with an enrichment factor of approximately 2, 5, and 50, respectively. The soil was rich in Al, Mn, and organic carbon with an approximate enrichment factor of 4, 2, and 6, respectively. Aqua-regia extraction associated with microwave digestion most likely underestimated the soil's total Fe and Al content due to the poor extractability of Fe phyllosilicates.[41] In contrast, Fe in the disposed filter-sand material primarily exists as short-range ordered (SRO) Fe(III) (oxyhydr)oxides[9,10] that are easily extractable with aqua regia.

Dynamics of Reactive Fe and As in Floodplain Soil and Disposed Filter-Sand Microcosms. As and Fe-rich sand filter materials are usually disposed onto floodplain soil or along the riverbank. To evaluate the potential for As mobilization from the filter-sand after disposal, we first incubated filter-sand and soil samples separately with ARW under reducing conditions. Within 130 days of incubation, the color changed from orange/gray to a darker black in the biotic microcosms, which is indicative of Fe(III) reduction (Figure S1). The highest Fe(III) reduction took place in the soil microcosms in which 0.5 M HCl-extractable Fe(II) increased from 0.008 to 4.6 g/kg sediment (Figure 1A). This equals to

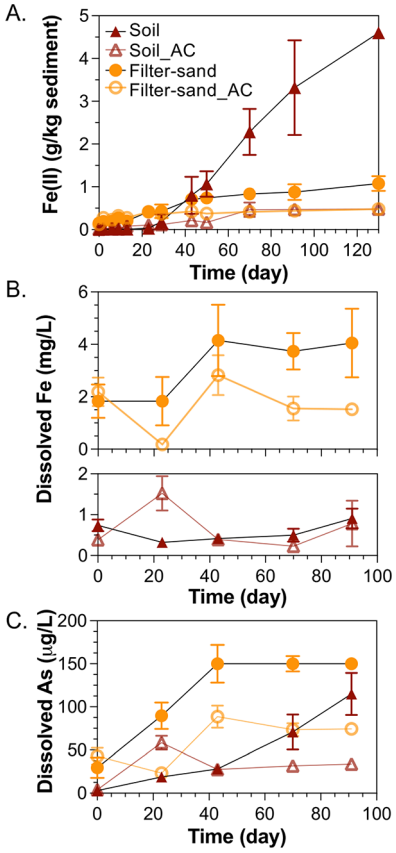

Figure 1. Changes in the concentration of 0.5 M HCl-extractable Fe(II) (A), dissolved Fe (B), and dissolved As (C) in floodplain soil, disposed filter-sand, and their abiotic control (AC) microcosms. All samples were analyzed in triplicate, and error bars indicate the standard deviation.

near-complete Fe(III) reduction from the 0.5 M HCl-extractable fraction (93 ± 8%) (Figure S2A). In comparison, microcosms with the filter-sand only displayed a limited extent of Fe(III) reduction in which the 0.5 M HCl-extractable Fe(II) increased from 0.15 to 1.1 g/kg sediment (Figure 1A). This equals a reduction of only 6 ± 1% of the poorly crystalline Fe pool (Figure S2A). Similar trends were observed in the 6 M-extractable Fe(II) and Fe(II)/Fe(total) ratios (Figures S2 and

https://doi.org/10.1021/acs.est.2c04915
Environ. Sci. Technol. 2022, 56, 16822−16830

S3, respectively), albeit with a lower magnitude of changes compared to the 0.5 M HCl-extractable fractions.

The dissolved total Fe was detected in small amounts in all microcosms; it increased from 2.0 to 4.2 mg/L in filter-sand microcosms. In contrast, the concentration remained around 0.7−0.9 mg/L in soil microcosms throughout the incubation (Figure 1B). Interestingly, even though the total As in the soil was lower relative to the disposed filter-sand, we detected the constant release of As from the soil to the aqueous phase from 3 to 115 μg/L over 130 days (Figure 1C). In comparison, the dissolved As in filter-sand microcosms increased sharply during the first 40 days to approximately 150 μg/L, which then leveled off until the end of the experiment (Figure 1C). Abiotic controls for both microcosms showed low levels of Fe(III) reduction and As mobilization, possibly due to abiotic processes or incomplete inhibition of microbial activity by NaN_3.[42] The 0.5 M HCl-extractable Fe(II) and dissolved As were < 0.5 g/kg and <60 μg/L, respectively, which were lower than the values observed in the experimental setups without microbial inhibition (Figure 1C).

Dynamics of Reactive Fe and As in the Microcosm Containing the Mixture of Filter-Sand and Soil. We hypothesized that, when the disposed filter-sand is mixed with soil, the microbial community and/or organic matter from the soil matrix may promote As mobilization from the disposed filter-sand by stimulating microbial Fe(III) and As(V) reduction. Therefore, we followed changes of reactive Fe and As in the mixture of filter-sand and soil microcosms (termed "sand−soil interaction") and compared them to a "no interaction" scenario. The values for the "no interaction" scenario were calculated by averaging the data obtained in soil-only and filter-sand-only microcosms as a method of applying a mass correction. This scenario, therefore, represents a hypothetical case that accounts for the mass of Fe and As in both the soil and filter-sand and implicitly assumes that the soil matrix plays no role in promoting or inhibiting Fe and As reduction.

By comparing the experimental sand−soil interaction case with the hypothetical "no interaction" case, we were able to clearly observe a promotive effect from the sand−soil interaction to Fe(III) and As(V) reduction, which overall led to about twice more As being mobilized compared to "no interaction". The content of 0.5 M HCl-extractable Fe(II) increased significantly in the mixture of the filter-sand and soil from 0.07 to 3.5 g/kg, which is 1.2 times higher than the "no interaction" case (Figure 2A). Similar trends were observed in the 6 M HCl-extractable Fe(II) and Fe(II)/Fe(total) ratios (Figures S2 and S3), albeit with a lower magnitude of changes compared to the 0.5 M HCl-extractable fractions.

The dissolved Fe concentration of the mixture microcosm was slightly lower than in the "no interaction" case. The dissolved Fe in the mixture of filter-sand and soil microcosms and abiotic control at day 0 (immediately after setup of the microcosm) was higher than on other days. We consider this to be an outlier, possibly due to short-term mixing effects between the soil and filter-sand materials. Disregarding these data points, the dissolved Fe gradually increased from 0.7 mg/L on day 23 to 2.1 mg/L but remained lower than in the "no interaction" case throughout the incubation period (Figure 2B).

Lastly, the dissolved As showed a marked increase in the mixture setup (up to 210 μg/L) relative to abiotic controls (maximum of 90 μg/L) and the "no interaction" scenario

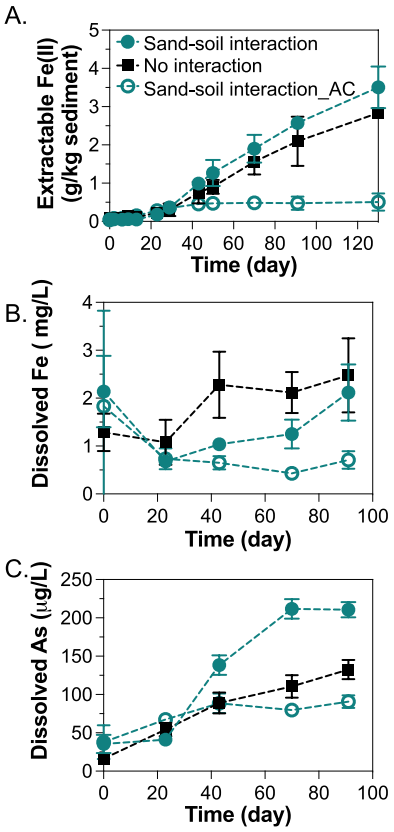

Figure 2. Comparison of Fe and As dynamics in the presence or absence of sand−soil interactions. Changes of poorly crystalline Fe (0.5 M HCl-extractable Fe), dissolved Fe, and As of the sand−soil interaction (mixture of filter-sand and soil) microcosms and their abiotic control (AC) microcosms are shown in A, B, C, respectively. The data is compared with corresponding value in the no-interaction case. The no-interaction value is calculated with values obtained from soil-only and filter-sand-only microcosms, assuming a 1:1 mixture and no promotion or inhibition effects. All samples were analyzed in triplicate, and error bars indicate the standard deviation.

(maximum of 120 μg/L) (Figure 2C). This means that As mobilization was promoted 1.8 times higher due to the sand−soil interaction than in the "no-interaction" case. Abiotic controls for the mixture microcosms showed lower levels of Fe(III) reduction and As mobilization overall (Figure 2).

Transformation of Fe Minerals in the Microcosms. Changes in Fe mineralogy can affect the fate of As and were therefore followed by Mössbauer spectroscopy. Fitting results and Mössbauer spectra collected at 5 and 77 K are shown in Table S2 and Figures S5−S7, respectively. The disposed filter-sand material prior to incubation consisted of 100% short-range-order (SRO) Fe(III) (oxyhydr)oxides (Figure 3A and Table S2), which was consistent with previous studies on sand filters.[9,10] After 100 days of incubation, there was up to 14% of Fe(II) in the filter-sand matrix (Figure 3A), equaling to a Fe(II)/Fe(III) ratio of 0.17 (Figure 3B), which is indicative of microbial Fe(III) reduction. In comparison, the soil initially contained a mixture of goethite (50%), low amounts of hematite (11%), Fe(III) phyllosilicates (25%), and Fe(II) (14%) (Figure 3A). The Fe(II) in the pre-incubation soil was likely in the form of phyllosilicates and not adsorbed Fe(II) as the soil had been sampled under oxic conditions. We observed an ∼6.3% increase in Fe(II) after 100 days in the soil incubations, equaling to a Fe(II)/Fe(III) ratio of 0.25 (Figure

https://doi.org/10.1021/acs.est.2c04915
Environ. Sci. Technol. 2022, 56, 16822−16830

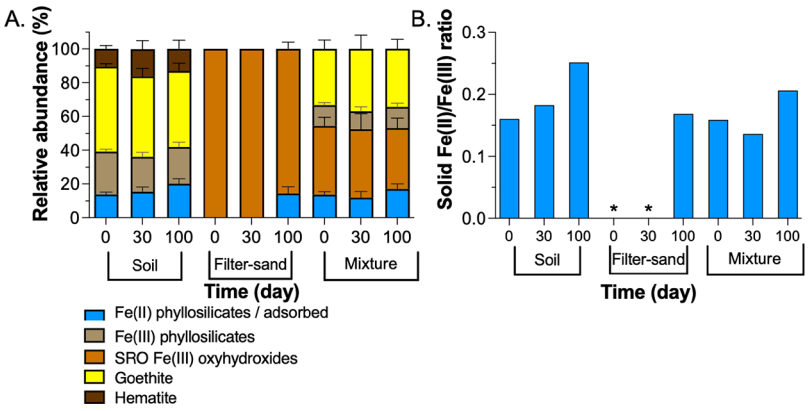

Figure 3. Fe mineralogy based on Mössbauer spectroscopy. Changes of the relative abundance of Fe minerals, measured temperature at 5 K (A), and ratio difference of Fe(II)/Fe(III) phases (B) over time in three different microcosms (soil, filter-sand, and the mixture of filter-sand and soil). (*) No Fe(II) detected in sand microcosms at days 0 and 30.

3B). Note that the increased Fe(II) observed based on spectra collected at 5 K may be slightly underestimated as the Fe(II) doublet can partially split at lower temperatures.[43] Based on the spectra collected at 77 K, the Fe(II) increased by 11% (Table S2). The mixture of filter-sand and soil microcosms showed Fe mineral distributions that reflect the end-member sand and soil with detectable levels of goethite, SRO Fe(III) (oxyhydr)oxides, and Fe(II) and Fe(III) phyllosilicates. We observed an increase of approximately 3.4% Fe(II) in the mixture setup after 100 days (Figure 3) based on the Mössbauer spectra at 5 K and 10% based on spectra collected at 77 K. We did not observe the formation of distinct Fe(II)-containing minerals such as magnetite or siderite.

In summary, we confirmed Fe(III) reduction in all microcosms. The filter-sand microcosm exhibited the highest relative increase in solid-phase Fe(II) over 100 days of incubation. This is because the filter-sand material consisted of nearly 100% (SRO) Fe(III) (oxyhydr)oxides in the form of two-line ferrihydrite,[9] which is more thermodynamically available for microbial reduction than hematite and goethite[44] found in soils.

Changes in the Solid-Phase As Redox State and Implications for As Binding Environment in the Microcosms. To determine changes in As redox states in the solid matrix, samples were analyzed at days 0, 30, and 84 by XANES and EXAFS at the As K edge using a linear combination fitting (LCF) approach (Figure 4 and Figures S8 and S9). XANES and EXAFS As speciation analyses showed comparable trends with minor differences in percentage contributions (Table S3). The arsenic redox distribution indicated that the disposed filter-sand and soil samples initially contained up to 90% As(V) and less than 10% As(III) (Figure 4A). After incubation, the As(III) contribution in sand microcosms increased by 23.6% of total As (Figure 4A). In the mixtures of the filter-sand and soil, As(III) was increased by 32% of the total As pool (Figure 4A), corresponding to an increase of As(III) from 41 to 273 mg/kg (Figure 4B).

Analysis of As EXAFS data suggested an As−Fe complex in all microcosms (at a distance of 2.88 Å radial structure function equaling to 3.3 Å in real distances) (Figure 4C), corresponding to As−Fe inner-sphere complexes dominated by a bidentate−mononuclear edge-sharing (^{2}E) formation on the surface of Fe(III) (oxyhydr)oxides.[45,46] This type of complex might result from As−O−O−As multiple scattering.[46−48] Overall, As K-edge EXAFS to the *k* of 12 was not able to

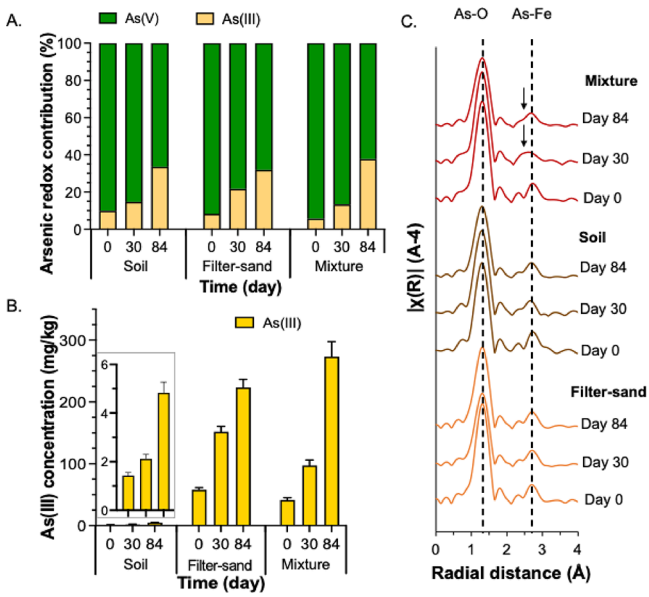

Figure 4. Changes of the As redox contribution obtained by LC fitting of XANES data (A), calculated solid-phase As(III) concentration combing XANES data and extraction data (B), and As K-edge EXAFS Fourier transform magnitude (C) over time in three different microcosms (soil, filter-sand, and mixture of filter-sand and soil). Arsenic EXAFS *k*3 graphs of samples are shown in Figure S8.

resolve outer-sphere As binding beyond 3.5 Å, which was more typically found above 5 Å.[49] Shell-by-shell fits did not show any clear trend for As coordination differences between the filter-sand, soil and sand−soil mixture (Table S4). On a more descriptive note, in the mixture samples at days 30 and 84 and not in the filter-sand-only or soil-only microcosms, a shift from 2.88 Å (3.3 Å in real distances) to a lower angstrom value was observed compared to day 0. This shift caused the 2.88 Å peak to be more diffused, suggesting that an outer-sphere As binding contribution possibly stemming of As mobilized from the disposed filter-sand material was now re-adsorbed in a slightly tighter coordination onto soils (arrows in Figure 4C).

Dynamics of Colloidal Fe and As in the Microcosms. In our microcosms, we observed colloids that regularly remained suspended near the top of the solution. This led us to investigate changes in Fe and As contents in the colloidal fraction as they can also be potentially mobilized and are

https://doi.org/10.1021/acs.est.2c04915
Environ. Sci. Technol. 2022, 56, 16822−16830

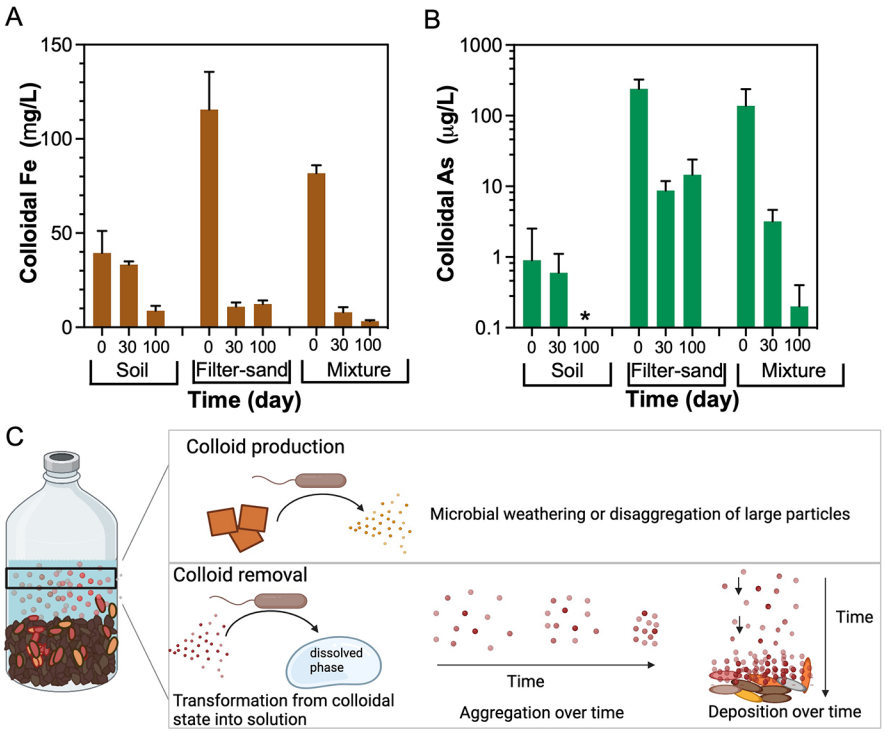

Figure 5. Changes in the colloidal mass concentration of Fe and As in microcosms (A, B) containing either the soil, disposed filter-sand, or the mixture of filter-sand and soil over time. All samples were analyzed in triplicate, and error bars indicate the standard deviation. (*) No colloidal As detected in soil microcosms at day 100. Schematic conceptualization of colloid production and removal in the microcosms is shown in C.

reactive. We investigated the changes of Fe and As in the colloidal fraction at three time points (days 0, 30, and 100) by single-particle ICP-MS (spICP-MS). Our previous work already showed a strong correlation between colloidal Fe and As but not with Al, suggesting that colloidal Fe is the main carrier of As instead of Al.[30]

Consistent with our expectation, the results indicated that the filter-sand material was the main source of colloidal Fe and As at day 0 with mass concentrations of 115 mg/L Fe and 240 μg/L As, respectively (Figure 5). These concentrations are much higher than those of dissolved Fe and As measured in the microcosms. In comparison, lower amounts of colloidal Fe and As were detectable in soil microcosms. The mixture of the filter-sand and soil had intermediate amounts of colloidal Fe and As in-between the unmixed filter-sand and soil microcosms. The colloidal Fe/As ratios were elevated by a factor of 5 to 141 compared to the microwave digestion-extractable fraction. This is likely due to the presence of small (but detectable) Fe-rich particles with As contents below the detection limit of spICP-MS (0.81 fg As/particle; Table S5), thus causing elevated colloidal Fe/As ratios. Over 100 days of incubation, we observed that colloidal Fe and As decreased over time. The most pronounced decrease was observed in the mixture microcosms in which over 90% of the colloidal mass was removed by the end (Figure 5).

Sand−Soil Interactions Promote Fe and As Reduction, Leading to As Mobilization. Our results indicated that open disposal of filter-sand and mixing with soils can promote microbial reduction and mobilization of As-bearing Fe(III) (oxyhydr)oxides. We propose three non-exclusive mechanisms that can explain this observation. First, sand materials provide Fe(III) minerals that are more reactive (e.g., ferrihydrite) compared to those found in soils (e.g., goethite, hematite). Microbial reduction rates of ferrihydrite are generally up to 2 orders of magnitude faster than for goethite and hematite that were in the soil samples.[44,50] Second, soil-associated organic carbon is likely to be more reactive than organic carbon associated with sand materials. During the flood season (June to October), massive amounts of organic-rich fluvial sediment are deposited in floodplain soils.[18,51] The soil organic carbon in the Red River delta was previously identified to be derived predominantly from a C_3/C_4 plant.[52] The water extractable fraction of this organic matter was shown to trigger microbial reduction of As-bearing Fe(III) (oxyhydr)oxides in the same sediments.[53] Last but not least, microbial input from the soil to the filter-sand can promote the activities of iron(III) and arsenic(V)-reducing bacteria in the final mixture. Iron-reducing bacteria such as *Shewanella* and *Geobacter* are common bacterial groups that are responsible for microbial reductive dissolution of As-bearing Fe(III) (oxyhydr)oxides in flooded soil.[54,55] Additionally, arsenate reducers are phylogenetically diverse and frequently present in paddy soils. They can directly reduce As(V) to toxic As(III) via dissimilation (ArrAB gene) or detoxification (*ars* gene) mechanisms.[54,56−58]

Colloidal Fe and As were observed in our system, suggesting that As mobilization in the form of colloids could be substantial. Colloids can form in the environment due to seasonal water table changes and physical perturbation such as heavy precipitation.[25,59,60] The production and removal mechanisms of colloids in the microcosms are schematized in Figure 5C. In our microcosms, colloids are produced by partial dissolution or disaggregation (weathering) of larger particles.[61] Conversely, colloids can be removed by (i) complete dissolution of colloidal particles and (ii) aggregation or deposition over time to form larger particles.[22,59] Despite high concentrations of colloids at the initial stages of our experiments, we observed a strong decrease in colloidal As and Fe over time. This indicates a lower risk of colloidal As

https://doi.org/10.1021/acs.est.2c04915
Environ. Sci. Technol. 2022, 56, 16822−16830

mobilization over time, and the removal of colloids is faster than their production in our experiments.

There are two possible reasons for this observation. First, since colloids are highly reactive and bioavailable, anaerobic bacteria might prefer Fe(III) and As(V) in the colloidal fraction to obtain energy for growth. Indeed, the reduction rate of Fe(III)-reducers such as *Geobacter* and *Shewanella* species are faster when supplied with small-sized Fe(III) (oxyhydr)-oxides.[27] Since the amount of colloidal Fe and As made up <1.2% of the total Fe and As extractable by aqua regia, a significant amount of colloids can be reduced without impacting the mass balance of the system.

Alternatively, since our microcosms were incubated standing with brief shaking only before sampling, there was ample time over the 100-day incubation period for aggregation and deposition of colloids to proceed. The stability of Fe colloids can be considered in terms of the C/Fe ratio of the systems. At low organic C/Fe ratios as found in our experiments (C/Fe < 0.2), colloidal Fe is not stabilized by organic matter.[62] Therefore, the colloids were more susceptible to forming larger aggregates.[62,63] This was followed by the deposition of the colloids by gravitational sedimentation over time with larger aggregates leading to faster deposition.[62]

ENVIRONMENTAL IMPLICATIONS

Our results indicated that a combined total of 116−390 μg/L of aqueous and colloidal As (0.3−4% of total As) was released from the solid phase. The remaining 96.0−99.7% of As was retained in the solid phases. In comparison, a recent estimate suggests that 100% of the As from open disposal will be mobilized to either soils or water over 100 years.[6] The comparison between our experiments and this model estimation is not direct, but our results would at least suggest that As can be retained in the original solid phases over a period of a few months. Therefore, we anticipate different implications of As remobilization from filter-sand materials. First, short-distance transport (centimeters to meters) can lead to As being retained primarily in the surrounding soils. This is not an immediate concern unless the soil is then used for agricultural purposes; in which case, this can lead to increased As content in consumable plants. Second, frequent flooding and anoxic conditions can lead to enhanced long-distance transport (e.g., kilometers) of As in the form of colloids and aqueous phases, entering water sources such as aquifers and rivers. This is especially bad if As is released into groundwater aquifers, wells, or rivers that are used for drinking water consumption and previously tested to have low As concentrations below the drinking water threshold. Thus, continuous testing is recommended for areas that utilize the open disposal method. The ultimate fate of remobilized As will need to be constrained in the context of flooding events[18] and the heterogeneous distribution of As in soils,[64] and these will have varying influences from site to site.

Redox fluctuations are particularly important in the field due to changes in the precipitation frequency throughout the year. Redox fluctuations can influence the crystallinity of Fe(III) (oxyhydr)oxides.[65] Ferrihydrite—the main host of As—can be transformed into more crystalline phases such as goethite or hematite as a result of redox fluctuations.[66] Additionally, redox fluctuations can promote organic carbon degradation in the aerobic zones near the surface, thus limiting the availability of organic carbon for anaerobic metabolisms at depth.[17] Incubation under cycled redox conditions is required in future experiments to understand changes in Fe mineralogy, organic carbon availability, and how these affect the release of colloidal and aqueous As.

ASSOCIATED CONTENT

Supporting Information

The Supporting Information is available free of charge at https://pubs.acs.org/doi/10.1021/acs.est.2c04915.

Description of microwave digestion, XAS and spICP-MS analysis, additional figures of extractable Fe(II)/Fe-(total) by 6 M HCl in all microcosms, fitting results of Mössbauer spectroscopy, As XANES, EXAFS, shell-by-shell fitting, and particle number concentration of Fe and As by spICP-MS (PDF)

AUTHOR INFORMATION

Corresponding Author

Muammar Mansor − *Geomicrobiology, Department of Geosciences, University of Tuebingen, 72076 Tuebingen, Germany;* orcid.org/0000-0001-7830-650X; Phone: +49 7071 29 78999; Email: muammar.muammar-bin-mansor@uni-tuebingen.de

Authors

Anh Van Le − *Geomicrobiology, Department of Geosciences, University of Tuebingen, 72076 Tuebingen, Germany*

E. Marie Muehe − *Plant Biogeochemistry, Department of Geosciences, University of Tuebingen, 72076 Tuebingen, Germany; Plant Biogeochemistry, Department of Environmental Microbiology, Helmholtz Centre for Environmental Research - UFZ, 04318 Leipzig, Germany*

Soeren Drabesch − *Geomicrobiology, Department of Geosciences, University of Tuebingen, 72076 Tuebingen, Germany*

Juan Lezama Pacheco − *Department of Earth System Science, Stanford University, Stanford, California 94305, United States*

Timm Bayer − *Geomicrobiology, Department of Geosciences, University of Tuebingen, 72076 Tuebingen, Germany*

Prachi Joshi − *Geomicrobiology, Department of Geosciences, University of Tuebingen, 72076 Tuebingen, Germany*

Andreas Kappler − *Geomicrobiology, Department of Geosciences and Cluster of Excellence: EXC 2124: Controlling Microbes to Fight Infection, University of Tuebingen, 72076 Tuebingen, Germany;* orcid.org/0000-0002-3558-9500

Complete contact information is available at: https://pubs.acs.org/10.1021/acs.est.2c04915

Author Contributions

A.K. obtained funding and conceptualized the study. Sampling campaigns, lab work, and manuscript writing were done by A.V.L. with support and feedback from M.M. and A.K. Sample preparation, measurement, and data analysis for XAS were done by J.L.P., E.M.M., and S.D. The Mössbauer spectra were collected by and analyzed by T.B. and P.J. The manuscript was revised by all co-authors.

Notes

The authors declare no competing financial interest.

https://doi.org/10.1021/acs.est.2c04915
Environ. Sci. Technol. 2022, 56, 16822−16830

■ ACKNOWLEDGMENTS

This work was funded by the German Research Foundation (DFG, no. KA1736/41-1). We thank M. Latimer for beamline support (proposal no. 5587). Use of the Stanford Synchrotron Radiation Lightsource, SLAC National Accelerator Laboratory, is supported by the U.S. Department of Energy, Office of Science, Office of Basic Energy Sciences under contract no. DE-AC02-76SF00515. The SSRL Structural Molecular Biology Program is supported by the DOE Office of Biological and Environmental Research and by the National Institutes of Health, National Institute of General Medical Sciences (including no. P41GM103393). The contents of this publication are solely the responsibility of the authors and do not necessarily represent the official views of NIGMS or NIH. A.V.L. acknowledges feedback from S.J. Hug for the manuscript and the help of P. Tutiyasarn and T. Schlereth for the sampling and experiment setup. A.K. acknowledges infrastructural support by the DFG under Germany's Excellence Strategy, Cluster of Excellence no. EXC2124, project ID no. 390838134. The graphical abstract was created with Bio Render.

■ REFERENCES

(1) Ippolito, J. A.; Barbarick, K. A.; Elliott, H. A. Drinking water treatment residuals : A review of recent uses. 2011, *2* (May 2010), 1−12, DOI: 10.2134/jeq2010.0242.

(2) Turner, T.; Wheeler, R.; Stone, A.; Oliver, I. Potential alternative reuse pathways for water treatment residuals: Remaining barriers and questions—a Review. *Water, Air, Soil Pollut.* **2019**, *230*, 1.

(3) Sullivan, C.; Tyrer, M.; Cheeseman, C. R.; Graham, N. J. D. Disposal of water treatment wastes containing arsenic - A review. *Sci. Total Environ.* **2010**, *408*, 1770−1778.

(4) Clancy, T. M.; Hayes, K. F.; Raskin, L. Arsenic waste management: A critical review of testing and disposal of arsenic-bearing solid wastes generated during arsenic removal from drinking water. *Environ. Sci. Technol.* **2013**, *47*, 10799−10812.

(5) Koley, S. Future perspectives and mitigation strategies towards groundwater arsenic contamination in West Bengal. India. *Environ. Qual. Manage.* **2022**, *31*, 75−97.

(6) Van Genuchten, C. M.; Etmannski, T. R.; Jessen, S.; Breunig, H. M. LCA of disposal practices for arsenic-bearing iron oxides reveals the need for advanced arsenic recovery. *Environ. Sci. Technol.* **2022**, 14109.

(7) Ghosh, A.; Mukiibi, M.; Ela, W. TCLP underestimates leaching of arsenic from solid residuals under landfill conditions. *Environ. Sci. Technol.* **2004**, *38*, 4677−4682.

(8) Islam, M. S.; Al Mamun, M. A.; Islam, M. N. Leachability of arsenic from wastes of arsenic removal units using modified toxicity characteristic leaching procedure. *J. Life Earth Sci.* **2012**, *6*, 19−26.

(9) Voegelin, A.; Kaegi, R.; Berg, M.; Nitzsche, K. S.; Kappler, A.; Lan, V. M.; Trang, P. T. K.; Göttlicher, J.; Steininger, R. Solid-phase characterisation of an effective household sand filter for As, Fe and Mn removal from groundwater in Vietnam. *Environ. Chem.* **2014**, *11*, 566−578.

(10) Nitzsche, K. S.; Lan, V. M.; Trang, P. T. K.; Viet, P. H.; Berg, M.; Voegelin, A.; Planer-Friedrich, B.; Zahoransky, J.; Müller, S. K.; Byrne, J. M.; Schröder, C.; Behrens, S.; Kappler, A. Arsenic removal from drinking water by a household sand filter in Vietnam - Effect of filter usage practices on arsenic removal efficiency and microbiological water quality. *Sci. Total Environ.* **2015**, *502*, 526−536.

(11) Van Le, A.; Straub, D.; Planer-Friedrich, B.; Hug, S. J.; Kleindienst, S.; Kappler, A. Microbial communities contribute to the elimination of As, Fe, Mn, and NH4+ from groundwater in household sand filters. *Sci. Total Environ.* **2022**, *838*, No. 156496.

(12) Winkel, L. H. E.; Trang, P. T. K.; Lan, V. M.; Stengel, C.; Amini, M.; Ha, N. T.; Viet, P. H.; Berg, M. Berg MArsenic pollution of groundwater in Vietnam exacerbated by deep aquifer exploitation for more than a century. *Proc. Natl. Acad. Sci. U. S. A.* **2011**, *108*, 1246−1251.

(13) Berg, M.; Stengel, C.; Trang, P. T. K.; Hung Viet, P.; Sampson, M. L.; Leng, M.; Samreth, S.; Fredericks, D. Magnitude of arsenic pollution in the Mekong and Red River Deltas - Cambodia and Vietnam. *Sci. Total Environ.* **2007**, *372*, 413−425.

(14) General Statistics Office of Vietnam. *The Vietnam population and housing census 2009—Age-sex structure and marital status of the population in Vietnam*. 2011.

(15) Hoang, A. T. P.; Prinpreecha, N.; Kim, K. W. Influence of mining activities on arsenic concentration in rice in Asia: A review. *Minerals* **2021**, *11*, 1−14.

(16) Ha, N. T. H.; Ha, N. T.; Nga, T. T. H.; et al. Uptake of arsenic and heavy metals by native plants growing near Nui Phao multi-metal mine, northern Vietnam. *Appl. Geochem.* **2019**, *108*, No. 104368.

(17) Stuckey, J. W.; Schaefer, M. V.; Kocar, B. D.; Benner, S. G.; Fendorf, S. Arsenic release metabolically limited to permanently water-saturated soil in Mekong Delta. *Nat. Geosci.* **2016**, *9*, 70−76.

(18) Connolly, C. T.; Stahl, M. O.; DeYoung, B. A.; Bostick, B. C. Surface flooding as a key driver of groundwater arsenic contamination in Southeast Asia. *Environ. Sci. Technol.* **2022**, *56*, 928−937.

(19) Oremland, R. S.; Stolz, J. F. The ecology of arsenic. *Science* **2003**, *300*, 939−944.

(20) Dixit, S.; Hering, J. G. Comparison of arsenic(V) and arsenic(III) sorption onto iron oxide minerals: Implications for arsenic mobility. *Environ. Sci. Technol.* **2003**, *37*, 4182−4189.

(21) Hassellov, M.; von der Kammer, F. Iron oxides as geochemical nanovectors for metal transport in soil-river systems. *Elements* **2008**, *4*, 401−406.

(22) Noël, V.; Kumar, N.; Boye, K.; Barragan, L.; Lezama-Pacheco, J. S.; Chu, R.; Tolic, N.; Brown, G. E.; Bargar, J. R. FeS colloids−formation and mobilization pathways in natural waters. *Environ. Sci. Nano* **2020**, *7*, 2102−2116.

(23) Montalvo, D.; Vanderschueren, R.; Fritzsche, A.; Meckenstock, R. U.; Smolders, E. Efficient removal of arsenate from oxic contaminated water by colloidal humic acid-coated goethite: Batch and column experiments. *J. Cleaner Prod.* **2018**, *189*, 510−518.

(24) Yao, Y.; Mi, N.; He, C.; Yin, L.; Zhou, D.; Zhang, Y.; Sun, H.; Yang, S.; Li, S.; He, H. Transport of arsenic loaded by ferric humate colloid in saturated porous media. *Chemosphere* **2020**, *240*, No. 124987.

(25) Ma, J.; Guo, H.; Weng, L.; Li, Y.; Lei, M.; Chen, Y. Distinct effect of humic acid on ferrihydrite colloid-facilitated transport of arsenic in saturated media at different pH. *Chemosphere* **2018**, *212*, 794−801.

(26) Fan, L.; Zhao, F.; Liu, J.; Frost, R. L. The As behavior of natural arsenical-containing colloidal ferric oxyhydroxide reacted with sulfate reducing bacteria. *Chem. Eng. J.* **2018**, *332*, 183−191.

(27) Mansor, M.; Xu, J. Benefits at the nanoscale: a review of nanoparticle-enabled processes favouring microbial growth and functionality. *Environ. Microbiol.* **2020**, *22*, 3633−3649.

(28) Bauer, M.; Blodau, C. Arsenic distribution in the dissolved, colloidal and particulate size fraction of experimental solutions rich in dissolved organic matter and ferric iron. *Geochim. Cosmochim. Acta* **2009**, *73*, 529−542.

(29) Gomez-Gonzalez, M. A.; Bolea, E.; O'Day, P. A.; Garcia-Guinea, J.; Garrido, F.; Laborda, F. Combining single-particle inductively coupled plasma mass spectrometry and X-ray absorption spectroscopy to evaluate the release of colloidal arsenic from environmental samples. *Anal. Bioanal. Chem.* **2016**, *408*, 5125−5135.

(30) Mansor, M.; Drabesch, S.; Bayer, T.; et al. Application of single-particle ICP-MS to determine the mass distribution and number concentrations of environmental nanoparticles and colloids. *Environ. Sci. Technol. Lett.* **2021**, 589.

(31) Schaedler, F.; Kappler, A.; Schmidt, C. A revised iron extraction protocol for environmental samples rich in nitrite and carbonate. *Geomicrobiol. J.* **2018**, *35*, 23−30.

(32) Viollier, E.; Inglett, P. W.; Hunter, K.; Roychoudhury, A. N.; Van Cappellen, P. The ferrozine method revisited: Fe (II)/Fe (III) determination in natural waters. *Appl. Geochem.* **2000**, *15*, 785−790.
(33) Stookey, L. L. Ferrozine—a new spectrophotometric reagent for iron. *Anal. Chem.* **1970**, *42*, 779−781.
(34) Lagarec, K.; Rancourt, D. G. Extended Voigt-based analytic lineshape method for determining N-dimensional correlated hyperfine parameter distributions in Mössbauer spectroscopy. *Nucl. Instrum. Methods Phys. Res., Sect. B* **1997**, *129*, 266−280.
(35) Muehe, E. M.; Obst, M.; Hitchcock, A.; Tyliszczak, T.; Behrens, S.; Schröder, C.; Byrne, J. M.; Michel, F. M.; Krämer, U.; Kappler, A. Fate of Cd during microbial Fe (III) mineral reduction by a novel and Cd-tolerant Geobacter species. *Environ. Sci. Technol.* **2013**, *47*, 14099−14109.
(36) Webb, S. M. SIXpack: a graphical user interface for XAS analysis using IFEFFIT. *Phys. Scr.* **2005**, *2005*, 1011.
(37) Ravel, B.; Newville, M. ATHENA, ARTEMIS, HEPHAESTUS: data analysis for X-ray absorption spectroscopy using IFEFFIT. *J. Synchrotron Radiat.* **2005**, *12*, 537−541.
(38) Muehe, E. M.; Morin, G.; Scheer, L.; Le Pape, P.; Esteve, I.; Daus, B.; Kappler, A. Arsenic(V) incorporation in vivianite during microbial reduction of arsenic(V)-bearing biogenic Fe(III) (oxyhydr)oxides. *Environ. Sci. Technol.* **2016**, *50*, 2281−2291.
(39) O'Day, P. A.; Rivera, N., Jr.; Root, R.; Carroll, S. A. X-ray absorption spectroscopic study of Fe reference compounds for the analysis of natural sediments. *Am. Mineral.* **2004**, *89*, 572−585.
(40) Cancés, B.; Juillot, F.; Morin, G.; Laperche, V.; Alvarez, L.; Proux, O.; Hazemann, J. L.; Brown, G. E.; Calas, G. XAS evidence of As (V) association with iron oxyhydroxides in a contaminated soil at a former arsenical pesticide processing plant. *Environ. Sci. Technol.* **2005**, *39*, 9398−9405.
(41) Raiswell, R.; Canfield, D. E.; Berner, R. A. A comparison of iron extraction methods for the determination of degree of pyritisation and the recognition of iron-limited pyrite formation. *Chem. Geol.* **1994**, *111*, 101−110.
(42) Bore, E. K.; Apostel, C.; Halicki, S.; Kuzyakov, Y.; Dippold, M. A. Soil microorganisms can overcome respiration inhibition by coupling intra-and extracellular metabolism: 13C metabolic tracing reveals the mechanisms. *ISME J.* **2017**, *11*, 1423−1433.
(43) Notini, L.; Latta, D. E.; Neumann, A.; Pearce, C. I.; Sassi, M.; N'Diaye, A. T.; Rosso, K. M.; Scherer, M. M. The role of defects in Fe (II)−goethite electron transfer. *Environ. Sci. Technol.* **2018**, *52*, 2751−2759.
(44) Kappler, A.; Bryce, C.; Mansor, M.; Lueder, U.; Byrne, J. M.; Swanner, E. D. An evolving view on biogeochemical cycling of iron. *Nat. Rev. Microbiol.* **2021**, *19*, 360−374.
(45) Fendorf, S.; Eick, M. J.; Grossl, P.; Sparks, D. L. Arsenate and chromate retention mechanisms on goethite. 1. Surface structure. *Environ. Sci. Technol.* **1997**, *31*, 315−320.
(46) Ona-Nguema, G.; Morin, G.; Juillot, F.; Calas, G.; Brown, G. E. EXAFS analysis of arsenite adsorption onto two-line ferrihydrite, hematite, goethite, and lepidocrocite. *Environ. Sci. Technol.* **2005**, *39*, 9147−9155.
(47) Manning, B. A.; Fendorf, S. E.; Goldberg, S. Surface structures and stability of arsenic(III) on goethite: Spectroscopic evidence for inner-sphere complexes. *Environ. Sci. Technol.* **1998**, *32*, 2383−2388.
(48) Sherman, D. M.; Randall, S. R. Surface complexation of arsenic(V) to iron(III) (hydr)oxides: Structural mechanism from ab initio molecular geometries and EXAFS spectroscopy. *Geochim. Cosmochim. Acta* **2003**, *67*, 4223−4230.
(49) Catalano, J. G.; Park, C.; Fenter, P.; Zhang, Z. Simultaneous inner-and outer-sphere arsenate adsorption on corundum and hematite. *Geochim. Cosmochim. Acta* **2008**, *72*, 1986−2004.
(50) Cutting, R. S.; Coker, V. S.; Fellowes, J. W.; Lloyd, J. R.; Vaughan, D. J. Mineralogical and morphological constraints on the reduction of Fe (III) minerals by Geobacter sulfurreducens. *Geochim. Cosmochim. Acta* **2009**, *73*, 4004−4022.
(51) Smedley, P. L.; Kinniburgh, D. G. A review of the source, behaviour and distribution of arsenic in natural waters. *Appl. Geochem.* **2002**, *17*, 517−568.
(52) Eiche, E.; Berg, M.; Hönig, S.-M.; Neumann, T.; Lan, V. M.; Trang, P. T. K.; Viet, P. H. Origin and availability of organic matter leading to arsenic mobilisation in aquifers of the Red River Delta, Vietnam. *Appl. Geochem.* **2017**, *77*, 184−193.
(53) Glodowska, M.; Stopelli, E.; Schneider, M.; Lightfoot, A.; Rathi, B.; Straub, D.; Patzner, M.; Duyen, V. T.; Berg, M.; Kleindienst, S.; Kappler, A. Role of in situ natural organic matter in mobilizing As during microbial reduction of FeIII-mineral-bearing aquifer sediments from Hanoi (Vietnam). *Environ. Sci. Technol.* **2020**, *54*, 4149−4159.
(54) Huang, J. H. Impact of microorganisms on arsenic biogeochemistry: A review. *Water, Air, Soil Pollut.* **2014**, *225*, 1.
(55) Corsini, A.; Cavalca, L.; Zaccheo, P.; Crippa, L.; Andreoni, V. Influence of microorganisms on arsenic mobilization and speciation in a submerged contaminated soil: Effects of citrate. *Appl. Soil Ecol.* **2011**, *49*, 99−106.
(56) Vaxevanidou, K.; Christou, C.; Kremmydas, G. F.; Georgakopoulos, D. G.; Papassiopi, N. Role of indigenous arsenate and iron (III) respiring microorganisms in controlling the mobilization of arsenic in a contaminated soil sample. *Bull. Environ. Contam. Toxicol.* **2015**, *94*, 282−288.
(57) Vaxevanidou, K.; Giannikou, S.; Papassiopi, N. Microbial arsenic reduction in polluted and unpolluted soils from Attica, Greece. *J. Hazard. Mater.* **2012**, *241-242*, 307−315.
(58) Zhu, Y. G.; Xue, X. M.; Kappler, A.; Rosen, B. P.; Meharg, A. A. Linking genes to microbial biogeochemical cycling: Lessons from arsenic. *Environ. Sci. Technol.* **2017**, *51*, 7326−7339.
(59) Kretzschmar, R.; Borkovec, M.; Grolimund, D.; Elimelech, M. Mobile subsurface colloids and their tole in contaminant transport. *Adv. Agron.* **1999**, *66*, 121−193.
(60) Zhao, J.; Chen, S.; Hu, R.; Li, Y. Aggregate stability and size distribution of red soils under different land uses integrally regulated by soil organic matter, and iron and aluminum oxides. *Soil Tillage Res.* **2017**, *167*, 73−79.
(61) Hochella, M. F., Jr.; Mogk, D. W.; Ranville, J.; Allen, I. C.; Luther, G. W.; Marr, L. C.; McGrail, B. P.; Murayama, M.; Qafoku, N. P.; Rosso, K. M.; Sahai, N.; Schroeder, P. A.; Vikesland, P.; Westerhoff, P.; Yang, Y. Natural, incidental, and engineered nanomaterials and their impacts on the Earth system. *Science* **2019**, *363*, No. eaau8299.
(62) Liao, P.; Li, W.; Jiang, Y.; Wu, J.; Yuan, S.; Fortner, J. D.; Giammar, D. E. Formation, aggregation, and deposition dynamics of nom-iron colloids at anoxic-oxic interfaces. *Environ. Sci. Technol.* **2017**, *51*, 12235−12245.
(63) Amstaetter, K.; Borch, T.; Kappler, A. Influence of humic acid imposed changes of ferrihydrite aggregation on microbial Fe(III) reduction. *Geochim. Cosmochim. Acta* **2012**, *85*, 326−341.
(64) Fakhreddine, S.; Prommer, H.; Scanlon, B. R.; Ying, S. C.; Nicot, J. P. Mobilization of arsenic and other naturally occurring contaminants during managed aquifer recharge: A critical review. *Environ. Sci. Technol.* **2021**, *55*, 2208−2223.
(65) Thompson, A.; Chadwick, O. A.; Boman, S.; Chorover, J. Colloid mobilization during soil iron redox oscillations. *Environ. Sci. Technol.* **2006**, *40*, 5743−5749.
(66) Kocar, B. D.; Fendorf, S. Thermodynamic constraints on reductive reactions influencing the biogeochemistry of arsenic in soils and sediments. *Environ. Sci. Technol.* **2009**, *43*, 4871−4877.

https://doi.org/10.1021/acs.est.2c04915
Environ. Sci. Technol. 2022, 56, 16822−16830